SNS-101, a monoclonal antibody that is highly selective for VISTA in the tumor microenvironment, demonstrates favorable pharmacokinetic and cytokine release characteristics and potentiates anti-PD-1 responsiveness

Thomas Thisted, Yuliya Kleschenko, Yoshiko Takeuchi*, Arnab Mukherjee, Zuzana Biesova, Anokhi Cifuentes, Robert H. Pierce, Robert D. Schreiber* & Edward H. van der Horst

Sensei Biotherapeutics, Inc., 451 D St, Boston, MA 02210

***Washington Univ. School Medicine, Dept. Pathology and Immunology, 425 South Euclid Ave, St. Louis, MO 63110**

INTRODUCTION

VISTA (V-domain Ig suppressor of T-cell activation) is an immune checkpoint, which suppresses T-cell activation and is highly expressed on myeloid cells, including macrophages and neutrophils[1]. Importantly, VISTA is only active at low pH (~pH 6) such as in the tumor microenvironment (TME) due to protonation of surface exposed histidine residues[2]. VISTA inhibition demonstrated excellent therapeutic potential in preclinical studies[3]. However, clinical development of anti-VISTA antibodies has been challenging due to three major factors: 1) lack of clarity on the identity of the critical counter-receptor responsible for T-cell suppression; 2) high clearance via target-mediated drug disposition (TMDD) by VISTA$^+$ neutrophils and monocytes at physiologic pH and; 3) cellular activation and cytokine release syndrome (CRS) at sub-therapeutic doses by engagement of VISTA in the blood.

OBJECTIVE

- To prevent TMDD and mitigate potential CRS we developed SNS-101, a human monoclonal IgG1 antibody specific for the protonated, active form of VISTA, and interrogated its inhibitory potential of VISTA interacting with proposed binding partners at low (6.0) and physiological pH (7.4)
- Potential for CRS was tested *in vitro* as well as *in vivo* in a humanized mouse model
- Pharmacokinetic (PK) profile and anti-tumor efficacy of SNS-101 in combination with anti-PD-1 was assessed in syngeneic tumor models utilizing target-expressing human VISTA knock-in (KI) mice

EXPERIMENTAL PROCEDURES

- VISTA binding to PSGL-1, VSIG-8, Syndecan-2, LRIG-1 and VSIG-3 was determined at pH 6.0 and pH 7.4 followed by competition with SNS-101
- CRS risk was evaluated in an *ex-vivo* system using circulating fresh human whole blood over a dose range between 1 µg/mL and 100 µg/mL and *in vivo* in human CD34$^+$ cord blood cells reconstituted BRGSF mice
- PK studies were conducted in human VISTA-KI mice and compared to wild type (target-null) mice
- Anti-tumor efficacy was assessed in VISTA-KI mice implanted with the syngeneic tumor models, MC38 and 1956
- SNS-101 was compared to JNJ, a clinical stage, non-pH-selective anti-VISTA antibody (variable region of JNJ-61610588[4] (now CI-8993) cloned onto human IgG1 backbone)

RESULTS

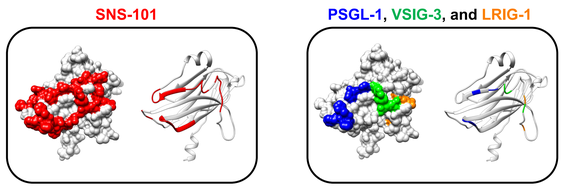

Figure 1. SNS-101 blocks PSGL-1:VISTA protein interface. Comparison of the putative SNS-101:VISTA binding interface (left; defined by peptide array binding (PepScan)) to the position of 5 key His residues involved in PSGL-1 binding[2], as well as residues proposed to be involved with binding of putative partners VSIG-3 and LRIG-1[5] (right). The human VISTA model from AlphaFold was used.

RESULTS

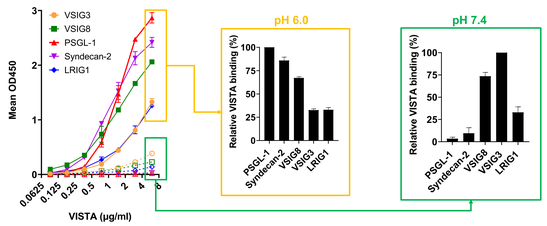

Figure 2. VISTA binds strongest to PSGL-1 at pH 6.0, but not at pH 7.4. Interaction between VISTA and PSGL-1 as well as 4 other putative receptors measured at pH 6.0 and 7.4 in an ELISA format. Wells were coated with 5 µg/ml of hVSIG3, hVSIG8, hPSGL-1, hSyndecan-2 or hLRIG1, and binding of biotinylated hVISTA-Fc using buffers at the respective pH values was detected by Streptavidin-HRP.

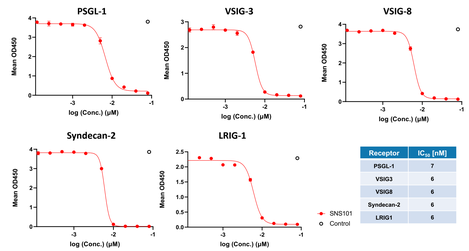

Receptor	IC_{50} [nM]
PSGL-1	7
VSIG3	6
VSIG8	6
Syndecan-2	6
LRIG1	6

Figure 3. SNS-101 inhibits VISTA:PSGL-1 interaction and all other potential binding partners. Similar to Figure 2, competition experiments were carried out at pH 6.0 with dilutions of SNS-101 or isotype control pre-incubated with 1 µg/ml of biotinylated hVISTA-Fc prior to addition to coated ELISA wells.

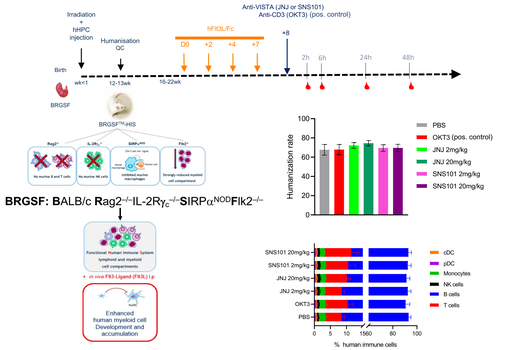

Figure 4. *In vivo* CRS model. BRGSF-HIS mice (reconstituted functional **h**uman **i**mmune **s**ystem) were generated as previously described[6]. BRGSF-HIS mice were quality controlled (QC) by assessing circulating human CD45$^+$ cells (top right) and specific immune cell subsets (lower right). Human myeloid cell development in BRGSF-HIS QC (n=60) mice was enhanced by intraperitoneal (IP) injection of hFlt3L-Fc. SNS-101 was compared to clinical stage, non-pH-selective anti-VISTA antibody JNJ. Serum was collected at indicated time points.

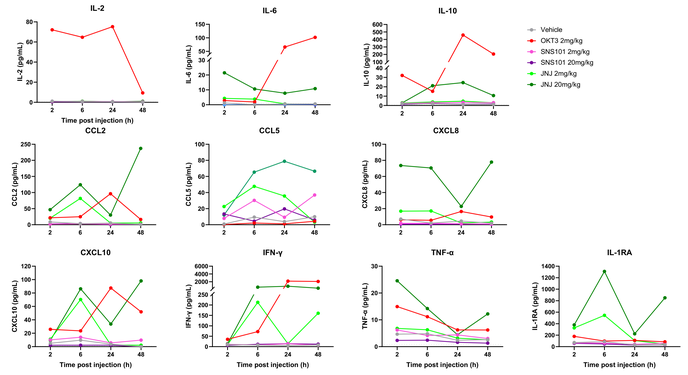

Figure 5. SNS-101 only mildly induces CCL-5 vs. dose-dependent induction of IL-6, IL-10, CCL-2 CCL-5, CXCL-8 CXCL-10, IFN-γ, TNF-α, and IL-1RA by JNJ. Serum of 6 mice per time point was collected and cytokines were quantified by a Multiplex bead-based assay. Positive control anti-CD3 (OKT3) efficiently induced CRS. Dotted line = detection limit.

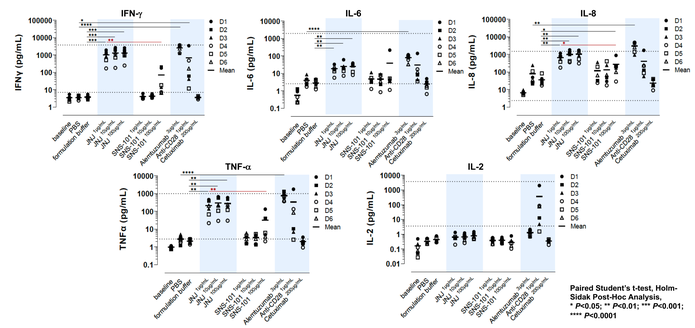

Figure 6. SNS-101 does not induce significant cytokine induction (IL-2, IL-6, IFN-γ, TNF-α) compared to JNJ. Circulating whole blood assay (ID.Flow) with six healthy donors was performed to predict CRS[7]. Plasma samples were collected at baseline and after 4h. Control antibodies alemtuzumab (pos. control), anti-CD28 (pos. control), and cetuximab (neg. isotype control) were compared to PBS, while JNJ and SNS-101-treated samples were compared to formulation buffer, and selected JNJ- and SNS-101-treated samples were compared to each other (indicated in red).

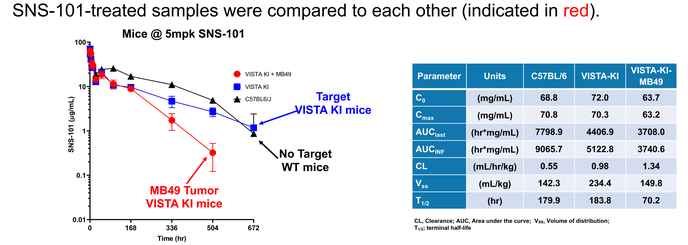

Parameter	Units	C57BL/6	VISTA-KI	VISTA-KI-MB49
C_0	(mg/mL)	68.8	72.0	63.7
C_{max}	(mg/mL)	70.8	70.3	63.2
AUC_{last}	(hr*mg/mL)	7798.9	4406.9	3708.0
AUC_{INF}	(hr*mg/mL)	9065.7	5122.8	3740.6
CL	(mL/hr/kg)	0.55	0.98	1.34
V_{ss}	(mL/kg)	142.3	234.4	149.8
$T_{1/2}$	(hr)	179.9	183.8	70.2

CL, Clearance; AUC, Area under the curve; V_{ss}, Volume of distribution; $T_{1/2}$, terminal half-life

Figure 7. SNS-101 shows linear elimination kinetics in target-bearing VISTA-KI mice vs. target-null mice and selective binding and target-mediated clearance in the TME of tumor-bearing VISTA-KI mice. Difference between the two VISTA groups illustrates the effect of the presence of tumor on the disposition of SNS-101. Mice (n=4) received IV bolus dose of SNS-101. Blood samples were collected over a 28-day period. Non-compartmental PK-parameters were estimated from the composite mean concentration versus time curves and are summarized in the table.

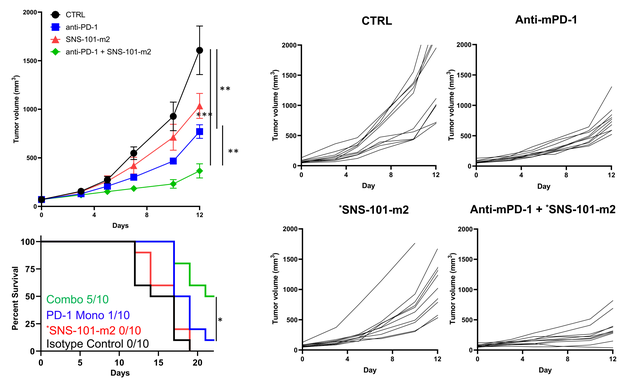

Figure 8. SNS-101 enhances anti-PD-1 response in MC-38 tumors. Mean tumor volumes (top left), spiderplots (right) and survival curves (lower left) are shown. 1 x 10^6 MC-38 were implanted into female VISTA-KI mice. Mice were randomized (n=8/cohort) once tumor volumes reached ~60-80 mm^3 and received IP injections every 3 days for 2 weeks (anti-mPD-1 mAb and SNS-101 were dosed at 5 mg/kg and 10 mg/kg, respectively).

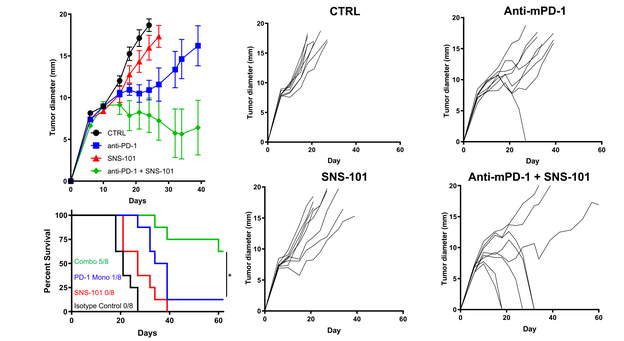

Figure 9. SNS-101 re-sensitizes anti-PD-1 insensitive 1956 sarcomas. Mean tumor diameters (top left), spiderplots (right) and survival curves (lower left) are shown. 1.5 x 10^6 1956 cells were implanted into female VISTA-KI mice. After 10 days, mice (n=8/cohort) received IP injections every 3 days (anti-mPD-1 and SNS-101 were dosed at 10 mg/kg and 20 mg/kg, respectively).

CONCLUSIONS

- SNS-101 potently inhibited the critical pH-dependent interaction between VISTA and PSGL-1, as well as interactions with other putative receptors
- *In vitro* and *in vivo* CRS assays suggest that SNS-101 has a significantly lower risk of inducing CRS than a non-pH-dependent VISTA antibody
- PK studies demonstrate that the pH-sensitive binding of SNS-101 avoided the rapid clearance by TMDD that has been observed with non-pH sensitive VISTA antibodies
- SNS-101 demonstrated significant enhancement of anti-tumor effects in combination with anti-PD-1 antibodies in multiple syngeneic tumor models
- Together, these data demonstrate that SNS-101's exquisite selectivity for active, protonated VISTA can abrogate TMDD and lower CRS risk, while significantly enhancing the anti-tumor effects of PD-1 blockade

1. Yuan *et al. Trends in Immunology* 42, (2021); 2. Johnston *et al. Nature* 574, (2019); 3. Gao *et al. Nature Medicine* 23, (2017); 4. Patent WO2017175058; 5. Thakkar *et al. J. Immunother Cancer* 10, (2022); 6. Lopez-Lastra *et al.* Blood Adv 10, (2017); 7. Fletcher *et al. Int Immunopharmacol.* 54, (2018)